

The Microstructure Evolution of Intrinsic Microcrystalline Silicon Films and Its Influence on the Photovoltaic Performance of Thin-Film Silicon Solar Cells *

Yuan Yujie^{1,2,3,†}, Hou Guofu^{1,2,3}, Zhang Jianjun^{1,2,3}, Xue Junming^{1,2,3},
Zhao Ying^{1,2,3}, and Geng Xinhua^{1,2,3}

(1 Institute of Photoelectronics, Nankai University, Tianjin 300071, China)

(2 Tianjin Key Laboratory of Photoelectronic Thin Film Devices and Technology, Tianjin 300071, China)

(3 Key Laboratory of Optoelectronic Information Science and Technology, Chinese Ministry of Education, Tianjin 300071, China)

Abstract: Hydrogenated microcrystalline silicon ($\mu\text{c-Si:H}$) intrinsic films and solar cells are prepared by plasma enhanced chemical vapor deposition (PECVD) with various hydrogen dilution ratios. The influence of hydrogen dilution ratios on electrical characteristics is investigated to study the phase transition from amorphous to microcrystalline silicon. During the deposition process, the optical emission spectroscopy (OES) from plasma is recorded and compared with the Raman spectra of the films, by which the microstructure evolution of different H_2 dilution ratios and its influence on the performance of $\mu\text{c-Si:H}$ n-i-p solar cells is investigated.

Key words: microcrystalline silicon; structure evolution; thin film silicon solar cells

PACC: 8115H; 8630J; 6855

CLC number: TM304

Document code: A

Article ID: 0253-4177(2008)11-2125-05

1 Introduction

Hydrogenated microcrystalline silicon ($\mu\text{c-Si:H}$) is receiving increased attention as the intrinsic absorber layer in the bottom cell of hydrogenated amorphous silicon (a-Si:H) based tandem solar cells^[1,2]. Although several methods have been employed to prepare $\mu\text{c-Si:H}$ ^[3~15], parallel plate plasma deposition, either from excitation frequencies in the radio-frequency (RF)^[6,7] or in the very-high-frequency (VHF)^[1,2,8] range, is the most successful technique for quality large-area material deposition.

The microstructure of $\mu\text{c-Si:H}$ is an important material property to influence the performance of solar cells. It was reported that the best conversion efficiency for $\mu\text{c-Si:H}$ solar cells is achieved with an intrinsic layer deposited near the $\mu\text{c-Si:H/a-Si:H}$ transition^[9], but such $\mu\text{c-Si:H}$ materials generally exhibit crystalline volume fraction increasing with film thickness and resulting in structural evolution along the growth axis^[8], leading to performance deterioration of the solar cell. Though the H_2 dilution profiling technique can partially control the structure homogeneity and improve the $\mu\text{c-Si:H}$ solar cell efficiency^[10], the mechanism is still unknown.

In this paper, plasma enhanced chemical vapor deposition (PECVD) is used for the preparation of $\mu\text{c-Si:H}$ films and solar cells. The influence of the hydrogen dilution ratio $R = [\text{H}_2]/[\text{SiH}_4]$ on the characteristics of $\mu\text{c-Si:H}$ is investigated in detail to study the physical mechanism of phase transition from amorphous to microcrystalline silicon. The gas phase species are *in situ* monitored by optical emission spectroscopy (OES) to characterize the film precursor density in the plasma. Previous research has shown that OES can be used as an effective tool to diagnose phase transition from amorphous to microcrystalline silicon^[11,12]. By comparing the Raman spectra of the films deposited at different R to the results of OES, the microstructure evolution of $\mu\text{c-Si:H}$ is analyzed thoroughly.

2 Experiment

The intrinsic $\mu\text{c-Si:H}$ films were deposited in an in-line seven-chamber RF glow discharge system at a plasma excitation frequency of 13.56MHz. Typical deposition parameters for the intrinsic layer are: base pressure of the vacuum chamber $p_{\text{base}} < 2.7 \times 10^{-4}$ Pa, deposition pressure $p = 400$ Pa, applied plasma power $P = 60$ W, and substrate temperature $T_s = 175^\circ\text{C}$. A gas

* Project supported by the State Key Development Program for Basic Research of China (Nos.2006CB202602,2006CB202603) and Tianjin Assistant Foundation for the National Basic Research Program of China (No.07QTPTJC29500)

† Corresponding author. Email: yjyuan@mail.nankai.edu.cn

Received 3 April 2008, revised manuscript received 20 July 2008

purifier was used to avoid incorporation of detrimental oxygen contamination. These conditions lead to deposition rates of $\sim 0.2\text{nm/s}$.

The $\mu\text{c-Si:H}$ single junction n-i-p solar cells were also fabricated to investigate the relativity between the devices and intrinsic films. In order to ensure that they have the same pre-seed layer during the film's deposition and device fabrication, an n-type $\mu\text{c-Si:H}$ coated glass was used as substrate to study the deposition of intrinsic $\mu\text{c-Si:H}$ materials. A series of intrinsic films with different thicknesses ranging from 50 to 1000nm was prepared for structural evolution research. Raman scattering measurements were carried out with a micro-Raman Renishaw spectrophotometer equipped with a cooled CCD detector and an argon laser excitation at 514nm. The crystalline volume fraction (X_c) of a sample is defined as: $X_c = (I_{500} + I_{520}) / (I_{480} + I_{500} + I_{520})$, in which $I_{500} + I_{520}$ is attributed to crystalline grains (at 500 and 520 cm^{-1}) and I_{480} is disordered regions (480 cm^{-1}). OES was used to characterize the plasma. The most attention was given to SiH^+ emission at 405~420nm and the hydrogen Balmer series of H_α at 656nm. The thicknesses of the intrinsic films were measured using an optical method.

The solar cells were constructed in the n-i-p sequence using SnO_2/ZnO coated glass as substrate. ITO/Al deposited on the p-layer served as the top contact and defined the solar cell area as 0.18 cm^2 . The solar cell performance was characterized by current density versus voltage (J - V) measurements under AM1.5 illumination (100 mW/cm^2), and solar energy conversion efficiency (Eff), fill factor (FF), open-circuit voltage (V_{oc}) and short-circuit current density (J_{sc}) were obtained from the J - V curve.

3 Results and discussion

3.1 Effect of hydrogen dilution ratio on electrical characteristics

In this section, a series of intrinsic Si:H films were prepared with different hydrogen dilution ratios, $R = [\text{H}_2] / [\text{SiH}_4]$, ranging from 32.33 to 99. The substrate was 7059 glass. The dark conductivity (σ_d) and photoconductivity (σ_{ph}) of these samples were measured, as shown in Fig.1. σ_d increased from $\sim 10^{-10}$ to $\sim 10^{-5}$ S/cm and σ_{ph} increased from $\sim 10^{-5}$ to $\sim 10^{-4}$ S/cm when R increased from 32.33 to 99, therefore the σ_{ph}/σ_d ratio of the films decreased from $\sim 10^4$ to $\sim 10^1$. The increase of σ_d with R is due to the structural changes of these films, especially when R is in the range from 44.45 to 46.6. The σ_d exhibited a

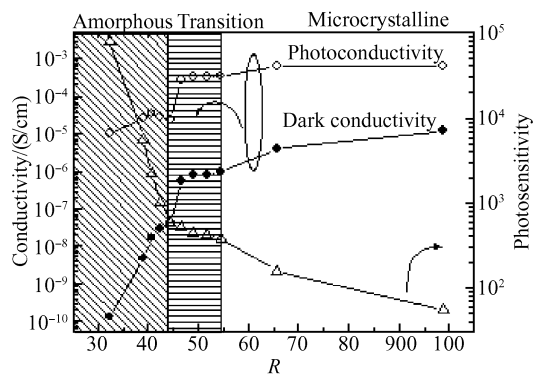


Fig.1 Conductivities and photosensitivities of intrinsic Si:H films deposited at various R

very sharp increase, which corresponded to an amorphous-to-microcrystalline transition. A good relationship can be found between the variation of σ_d and structural evolution. That is to say, the variation of σ_d can also diagnose the transition region from a-Si:H to $\mu\text{c-Si:H}$, so we can primarily estimate that amorphous silicon was obtained in the range of $R < 44.45$ and microcrystalline silicon was obtained in the range of $R > 54.55$. Our investigation placed emphasis on the range of $44.45 \leq R \leq 54.55$, corresponding to the transition region.

3.2 Effect of hydrogen dilution ratio on structural characteristic

To investigate the effect of the H_2 dilution ratio R on structure of Si:H i-layers, a series of intrinsic films with different thicknesses ranging from 50 to 1000nm was prepared. Glass coated with an n-type $\mu\text{c-Si:H}$ seed layer was used as the substrate. We deposited Si:H i-layers under the condition close to the transition region from $\mu\text{c-Si:H}$ to a-Si:H growth.

We employed the depth-profiled Raman spectroscopy to investigate the gradient in film crystallinity. Figure 2 shows the crystallinity profiles of $\mu\text{c-Si:H}$ deposited with different H_2 dilution ratios. The crystallinity increased clearly with the film thickness

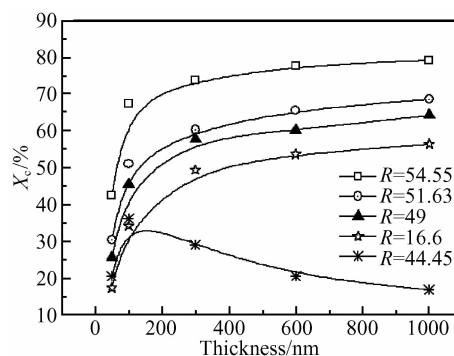


Fig.2 Crystalline volume fraction (X_c) as a function of thickness for various H_2 dilution ratios R

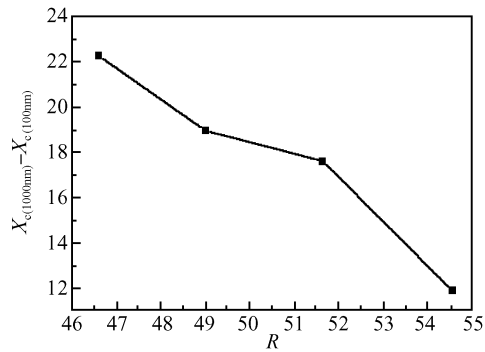


Fig.3 $X_{c(1000nm)} - X_{c(100nm)}$ as a function of H₂ dilution ratio R

when $R \geq 46.6$. Generally, a low H₂ dilution such as $R = 44.45$ leads to an amorphous growth of the film. However, under the condition of $R = 44.45$, there is an increase in crystallinity for the initial 100nm of the film, and then a decrease for the last part of the film. This could be explained by epitaxy growth of the i-layer deposited on the highly crystallized n-layer, therefore causing a positive crystallinity gradient in the first part of the film. The following decrease of crystallinity is due to a higher amorphous composition in the last part of the film.

The values of $X_{c(1000nm)} - X_{c(100nm)}$ are plotted as a function of R in Fig. 3. This figure shows that the value of $X_{c(1000nm)} - X_{c(100nm)}$ decreases as R increases. This means that the $\mu\text{c-Si:H}$ structural evolution becomes more inhomogeneous as R decreases from 54.55 to 46.6.

In fact, it has been proven that the material's structural and opto-electrical characteristic is determined during the deposition process^[11,12,14]. In order to get more information during the deposition and then compare with the Raman spectra of the films to investigate microstructure evolution of different R , the OES from the plasma were monitored for 50min as the H₂ dilution ratio R increases from 44.45 to 54.55.

The intensities of SiH* and H_α/SiH* ratios are plotted as a function of deposition time for different R in Figs. 4 and 5. Figure 4 shows that under all conditions, the SiH* emission intensity decreases during deposition, and the SiH* signal shows a more distinct decrease within the first minutes. The drop taking place within the first minutes is distinctively stronger for the low H₂ dilution ratio sample condition. The decrease of SiH* emission indicates a decrease of SiH₄ density, in other words, a depletion of SiH₄^[11]. The effect on the deposited film is that, due to the decreasing of SiH₄ content in the plasma, a "transient depletion" that induced amorphous incubation layer is formed^[11]. Growth on this amorphous incubation layer will introduce a positive crystallinity gradient in

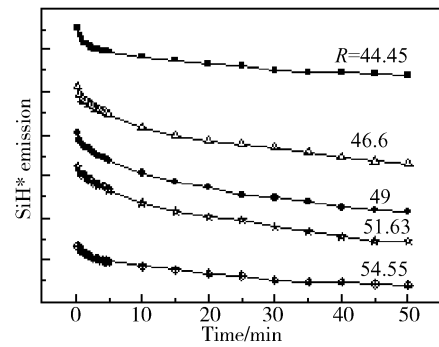


Fig.4 SiH* emission at 414nm during $\mu\text{c-Si:H}$ absorber layer growth with H₂ dilution ratio close to the transition to amorphous growth

the deposited film, as was shown by Collins *et al.*^[13].

The intensity of SiH* and H_α implies the amount of growth precursor and atomic hydrogen respectively, so the H_α/SiH* ratio can be used to evaluate the relative concentration of atomic hydrogen and SiH_n ($n = 1, 2, 3$) in the plasma^[12]. Figure 5 shows that when $R \geq 46.6$, the H_α/SiH* ratio increases during deposition and the ratio exhibits a sharp increase within the first minutes. The upward slope in the ratio H_α/SiH* is particularly large for the low H₂ dilution ratio condition, implying that the $\mu\text{c-Si:H}$ structural evolution becomes more inhomogeneous as R decreases from 54.55 to 46.6. This result is in accordance with the Raman spectra. For the $R = 44.45$ condition, the H_α/SiH* ratio increases within the first minutes and then tends to be saturated. This is because the H₂ dilution ratio $R = 44.45$ is just below the transition region, and the relative concentration of the produced species in the plasma has changed, as shown by Hou *et al.*^[12].

3.3 Effect of hydrogen dilution ratio on solar cells

Solar cells are very sensitive to changes in structural or optoelectronic properties of the $\mu\text{c-Si:H}$ film. Therefore, $\mu\text{c-Si:H}$ n-i-p solar cells were fabricated to evaluate the qualities of intrinsic $\mu\text{c-Si:H}$ layers de-

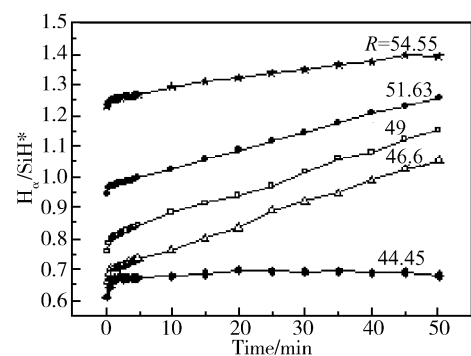


Fig.5 Ratio of H_α/SiH* during $\mu\text{c-Si:H}$ absorber layer growth with H₂ dilution close to the transition to amorphous growth

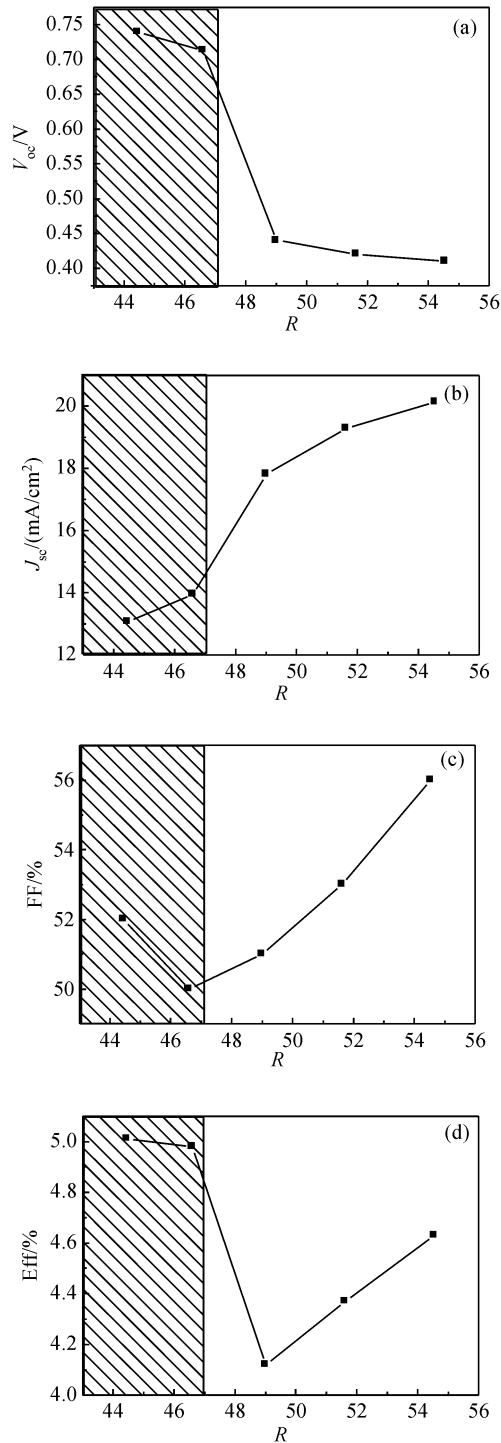


Fig.6 Solar cell parameters open-circuit voltage V_{oc} , short-circuit current J_{sc} , fill-factor FF, and efficiency Eff as function of H_2 dilution ratio

posited at various H_2 dilution ratios R with an i-layer thickness of $1.0 \pm 0.1 \mu\text{m}$. SnO_2/ZnO coated glass substrates served as back contacts, while ITO/Al deposited on the p-layer served as the top contact and defined the solar cell area of 0.18cm^2 . The deposition conditions for intrinsic $\mu\text{c-Si:H}$ film were the same as those of samples in Fig. 1.

Figure 6 shows the solar cell properties obtained at various H_2 dilution ratio R . For the sample with H_2

dilution ratio $R \leq 46.6$ condition, the higher V_{oc} and lower J_{sc} indicate a lower average microcrystalline volume fraction in the i-layer. However, Figures 1 and 2 indicate that the intrinsic material shows $\mu\text{c-Si:H}$ characteristics for the $R = 46.6$ condition. This is mainly due to the substrate influence.

For the $R > 46.6$ condition, the V_{oc} decreases and the J_{sc} increases as the H_2 dilution ratio increases, which implies the average microcrystalline volume fraction (X_c) in the i-layer increases. This result is in accordance with the crystallinity in Fig. 2. The fill-factor (FF) increases as the H_2 dilution ratio increases. This could be explained by the $\mu\text{c-Si:H}$ structural evolution getting more serious and the amorphous incubation layer becoming thicker with lower R (see Figs. 2~5) for the $R \leq 46.6$ condition, which would induce a poorer carrier transport.

4 Conclusion

The influence of the H_2 dilution ratio on the electrical and structural characteristics of $\mu\text{c-Si:H}$ were investigated in detail. The results show that both Raman spectra and optical emission spectroscopy can detect the structural variation of materials. The $\mu\text{c-Si:H}$ structure evolution gets more serious and the amorphous incubation layer becomes thicker when the intrinsic layer is deposited near the edge of the transition region from $\mu\text{c-Si:H}$ to a-Si:H , which induces a poorer carrier transport and leads to poorer solar cell performance.

References

- [1] Meier J, Dubail S, Platz R, et al. Towards high-efficiency thin-film silicon solar cells with the "micromorph" concept. *Solar Energy Materials and Solar Cells*, 1997, 49(1~4): 35
- [2] Vetterl O, Finger F, Carius R, et al. Intrinsic microcrystalline silicon: a new material for photovoltaics. *Solar Energy Materials and Solar Cells*, 2000, 62(1/2): 97
- [3] Mai Y, Klein S, Geng X, et al. Differences in the structure composition of microcrystalline silicon solar cells deposited by HWCVD and PECVD: influence on open circuit voltage. *Thin Solid Films*, 2006, 501(1/2): 272
- [4] Smit C, Hamers E, Korevaar B, et al. Fast deposition of microcrystalline silicon with an expanding thermal plasma. *Journal of Non-Crystalline Solids*, 2002, 299~302: 98
- [5] Kosku N, Murakami H, Higashi H, et al. Influence of substrate DC bias on crystallinity of silicon films grown at a high rate from inductively-coupled plasma CVD. *Appl Surf Sci*, 2005, 244(1~4): 39
- [6] Takai M, Nishimoto T, Takagi T, et al. Guiding principles for obtaining stabilized amorphous silicon at larger growth rates. *J Non-Cryst Solids*, 2000, 266~269: 90
- [7] Rech B, Repmann T, Donker M, et al. Challenges in microcrystalline silicon based solar cell technology. *Thin Solid Films*, 2006, 511/512: 548

- [8] Liu Y, Rath J, Schropp R. Development of micromorph tandem solar cells on foil deposited by VHF-PECVD. *Surface and Coatings Technology*, 2007, 201(22/23): 9330
- [9] Edelman F, Chack A, Weil R. Structure of PECVD Si:H films for solar cell applications. *Solar Energy Materials and Solar Cells*, 2003, 77(2): 125
- [10] Yan B, Yue G, Guha S. Status of nc-Si:H solar cells at united solar and roadmap for manufacturing a-Si:H and nc-Si:H based solar panels. *Mater Res Soc Symp Proc*, 2007: 989
- [11] Donker M, Kilper T, Grunsky D, et al. Microcrystalline silicon deposition: process stability and process control. *Thin Solid Films*, 2007, 515(19): 7455
- [12] Hou G F, Xue J M, Yuan Y J, et al. A fast method to diagnose phase transition from amorphous to microcrystalline silicon. *Sci China Ser G-Phys Mech Astron*, 2007, 50: 731
- [13] Collins R, Ferlauto A, Ferreira G, et al. Evolution of microstructure and phase in amorphous, protocrystalline, and microcrystalline silicon studied by real time spectroscopic ellipsometry. *Solar Energy Materials and Solar Cells*, 2003, 78(1~4): 143
- [14] Hou G F, Xue J M, Guo Q C, et al. Formation mechanism of incubation layers in the initial stage of microcrystalline silicon growth by PECVD. *Chinese Physics*, 2007, 16: 553

本征微晶硅薄膜的结构演变及其对太阳能电池光伏性能的影响*

袁育杰^{1,2,3,†} 侯国付^{1,2,3} 张建军^{1,2,3} 薛俊明^{1,2,3} 赵颖^{1,2,3} 耿新华^{1,2,3}

(1 南开大学光电子薄膜器件与技术研究所, 天津 300071)

(2 光电信息技术科学教育部重点实验室, 天津 300071)

(3 光电子薄膜器件与技术天津市重点实验室, 天津 300071)

摘要: 采用高压射频等离子体增强化学气相沉积(RF-PECVD)方法制备本征硅薄膜和 n-i-p 结构太阳能电池, 研究了氢稀释率对本征硅薄膜的电学特性和结构特性的影响. 采用光发射谱(OES)和喇曼(Raman)散射光谱研究了处于过渡区的本征硅薄膜的纵向结构演变过程. 结果表明: 光发射谱和喇曼散射光谱可以作为研究硅薄膜的纵向结构演变有效手段. 随着氢稀释率的增加, 硅薄膜从非晶相向微晶相过渡时, 其纵向结构的改变会严重影响硅薄膜太阳能电池的光伏性能.

关键词: 微晶硅; 结构演变; 硅薄膜太阳能电池

PACC: 8115H; 8630J; 6855

中图分类号: TM304 **文献标识码:** A **文章编号:** 0253-4177(2008)11-2125-05

* 国家重点基础研究发展计划(批准号:2006CB202602,2006CB202603)和国家科技计划配套项目(批准号:07QTPTJC29500)资助项目

† 通信作者. Email: yjyuan@mail.nankai.edu.cn

2008-04-03 收到, 2008-07-20 定稿